

PACS numbers: 42.55.Px; 42.60.Lh; 42.81.Qb; 42.79.Dj; 42.79.Sz
DOI: 10.1070/QE2013v043n10ABEH015028

S–C–L triple wavelength superluminescent source based on an ultra-wideband SOA and FBGs

H. Ahmad, M.Z. Zulkifli, N.A. Hassan, F.D. Muhammad, S.W. Harun

Abstract. **We propose and demonstrate a wide-band semiconductor optical amplifier (SOA) based triple-wavelength superluminescent source with the output in the S-, C- and L-band regions. The proposed systems uses an ultra-wideband SOA with an amplification range from 1440 to 1620 nm as the linear gain medium. Three fibre Bragg gratings (FBGs) with centre wavelengths of 1500, 1540 and 1580 nm are used to generate the lasing wavelengths in the S-, C- and L-bands respectively, while a variable optical attenuator is used to finely balance the optical powers of the lasing wavelengths. The ultra-wideband SOA generates an amplified spontaneous emission (ASE) spectrum with a peak power of –33 dBm at the highest SOA drive current, and also demonstrates a down-shift in the centre wavelength of the generated spectrum due to the spatial distribution of the carrier densities. The S-band wavelength is the dominant wavelength at high drive currents, with an output power of –6 dBm as compared to the C- and L-bands, which only have powers of –11 and –10 dBm, respectively. All wavelengths have a high average signal-to-noise ratio more than 60 dB at the highest drive current of 390 mA, and the system also shows a high degree of stability, with power fluctuations of less than 3 dB within 70 min. The proposed system can find many applications where a wide-band and stable laser source is crucial, such as in communications and sensing.**

Keywords: *ultra-wideband semiconductor optical amplifier, S-, C-, L-band superluminescent source.*

1. Introduction

Multi-wavelength fibre lasers (MWFLs) have recently attracted significant interest as compact and cost-effective transmission sources for a variety of applications in optical communications [1–3], optical sensing [4, 5], optical instrumentation [6] and even microwave photonic systems [7]. Conventionally, erbium doped fibres (EDFs) are employed as the gain media for MWFLs due to their large gain, high saturation power and relatively low noise figure, thus generating high quality signals.

Currently, most EDF-based MWFLs are optimised to operate at the C-band region of 1530 nm to 1565 nm [8]. However, the recent expansion of the communications bandwidth into the L-band region of 1565 nm to 1625 nm has necessitated the development of cost effective wavelength sources for this bandwidth. For the EDF-based MWFL to operate at the L-band region, an additional length of an EDF must be added to the MWFL. The drawback of this approach is the lower gain and higher noise figure encountered by the system, thereby reducing the overall quality of the lasing wavelength generated [9, 10]. Furthermore, the simultaneous lasing of both C- and L-band signals in the MWFL cannot be achieved by conventional means, and requires special techniques such as the four-wave-mixing effect [11] or the use of specialty fibres such as bismuth-doped fibres [12] and highly nonlinear fibres [13] as well as complex configurations such as an EDF-Raman hybrid [14]. In addition, researchers are now looking towards the S-band region of 1480 nm to 1530 nm for future transmission needs, and S-band MWFLs have therefore attracted significant interest as low-cost sources for transmission in the S-band region. However, as was the case with the L-band MWFL, the S-band MWFL cannot be implemented by conventional means, and requires specialised fibres such as depressed-cladding EDFs [15] or special techniques such as Brillouin scattering [16] in order to generate lasing wavelengths. As a result, it is very difficult to develop an ultra-wideband MWFL capable of generating simultaneous lasing wavelengths in the S-, C- and L-band regions using a single gain medium.

Besides MWFLs, there is also a need for multi-wavelength superluminescent sources (MWSS) that can find useful applications in the areas of sensors and also act as a source of probe signals for the S-, C- and L-bands. This will complement the existing fibre lasers and provide a low-cost, ultra-wideband signal source. The semiconductor optical amplifier (SOA) is a highly suitable candidate for the generation of an ultra-wide band MWSS, particularly because of its inhomogeneous broadening properties. Unlike the EDF, which has homogenous broadening properties, the SOA allows for the simultaneous amplification of multiple wavelengths without the detrimental effects of mode-competition and unstable signal outputs, covering a range of 1440 nm to 1620 nm. This range covers the S-, C- and L-bands and allows for the development of compact and low cost SOA-based MWSS without the need for complex configurations or special techniques.

In this work, a triple wavelength MWSS is proposed and demonstrated utilising an ultra-wideband SOA as the linear gain medium and fibre Bragg gratings with centre wavelengths of 1500, 1540 and 1580 nm, respectively, as wavelength filters for the simultaneous generation of the S-, C- and L-band superluminescent outputs. The proposed system is analysed for its performance in terms of power and signal-to-noise ratio (SNR), and also for its stability over extended periods of time. The proposed triple-wavelength MWSS will have many potential applications in communications and sensing tasks.

H. Ahmad, M.Z. Zulkifli, N.A. Hassan, F.D. Muhammad, S.W. Harun
Photonics Research Centre, University of Malaya, 50603 Kuala Lumpur, Malaysia; e-mail: harith@um.edu.my;

Received 24 October 2012; revision received 31 March 2013
Kvantovaya Elektronika **43** (10) 923–926 (2013)
Submitted in English

2. Experimental setup

Figure 1 shows the experimental setup of the proposed S–C–L MWSS. The MWSS consists of two main components: a ring cavity which provides gain for the superluminescent output and a filtering mechanism to obtain the S-, C- and L-wavelengths.

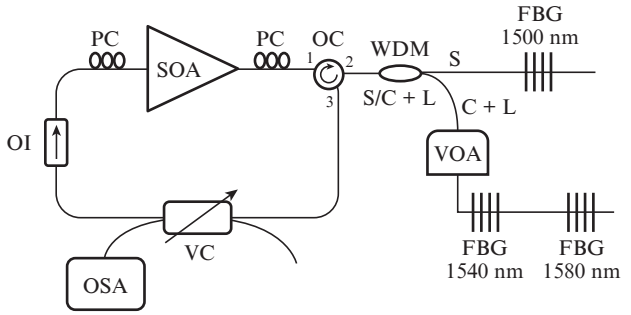

Figure 1. Experimental setup for a triple wavelength S–C–L-band superluminescent source:
(PC) polarisation controller; (OC) optical circulator; (WDM) wavelength division multiplexer; (OI) optical isolator; (VOA) variable optical attenuator; (VC) variable coupler; (OSA) optical spectrum analyser.

The gain medium of the S–C–L MWSS is an ultra-wideband SOA, with an amplification bandwidth of more than 220 nm from 1400 nm to 1620 nm. The active layer of the SOA is an InGaAsP substrate, which provides a gain bandwidth of 160 nm and a polarisation dependent gain of 1.5 dB. Initially, the SOA generates the amplified spontaneous emission (ASE) spectrum, which then travels from the output of the SOA through a polarisation controller (PC) and then to port 1 of the optical circulator (OC). The ASE spectrum is then emitted at port 2 of the OC, where it now encounters the common port of an S/C + L wavelength division multiplexer (WDM). Here, the ASE spectrum is split into two spectral components, with one spectral component covering the S-band region, while the second spectral component covering the C- and L-band regions. The S-band spectrum is channelled to a 1500-nm fibre Bragg grating (FBG), which reflects only a single superluminescent output at a wavelength of 1500 nm. The FBG has a reflectivity of 99%, with a spectrum width of about 1.5 nm (Fig. 2), which is shown for wavelength of 1500 nm. A similar profile is seen for wavelengths of 1540 and 1580 nm.

In the same manner, the second spectral component (which is the C- and L-band) is channelled through a variable optical attenuator (VOA) towards two FBGs, which reflect two superluminescent wavelengths at 1540 and 1580 nm. The VOA is used to control the power of the two superluminescent wavelengths at 1540 nm and 1580 nm so that it is the same as that of the 1500-nm signal. The VOA is used to allow for power adjustments because there is a tendency of having a higher oscillation power in the C- and L-band region, even though peak ASE of the SOA is higher in the S-band region. The reflected signals at 1500, 1540 and 1580 nm now travel to the S/C + L WDM and are combined to form a triple superluminescent wavelength spectrum which then travels towards port 2 of the OC, which is then emitted at port 3. This triple wavelength will then oscillate in the ring cavity through the 2×2 variable coupler (VC) and the optical isolator (OI), which will force the oscillation in a clock-wise direction as well as another PC. The variable coupler will allow for different coupling ratios, where a portion of the oscillating signal is then extracted for analysis using an optical spectrum analyser (OSA) with a resolution of 0.02 nm.

3. Result and discussions

Figure 3 shows the ASE spectra of the ultra-wideband SOA at different drive currents. As can be seen, the power of the ASE spectrum obtained at a drive current of 70 mA forms a bell shape, rising gently from approximately –65 dBm at 1440 nm to a peak value of about –49 dBm at 1540 nm, before slowly decreasing to –60 dBm at a wavelength of 1620 nm. As the drive current increases to 150 mA, the same spectral shape is obtained, rising from –54 dBm at 1440 nm to –40 dBm at 1507 nm before dropping to about –57 dBm at 1620 nm. At 270 mA, the ASE spectrum obtained has a power of –45 dBm at 1440 nm, rising to –35 dBm at 1492 nm before dropping again to –55 dBm at 1620 nm, while at the highest drive current of 390 mA, the spectrum obtained has a power of –41 dBm at 1440 nm, rising to –33 dBm at 1486 nm before dropping again to approximately –55 dBm at 1620 nm.

From the spectra of Fig. 3, two important observations can be made, which will in turn determine the behaviour of the superluminescent source during the later stages of this work. The first observation is that at lower drive currents, a

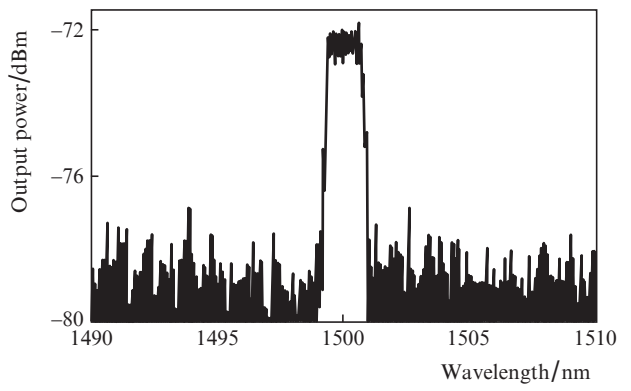

Figure 2. FBG reflectivity at 1500 nm, having a linewidth of about 1.5 nm and a reflectivity close to 99%.

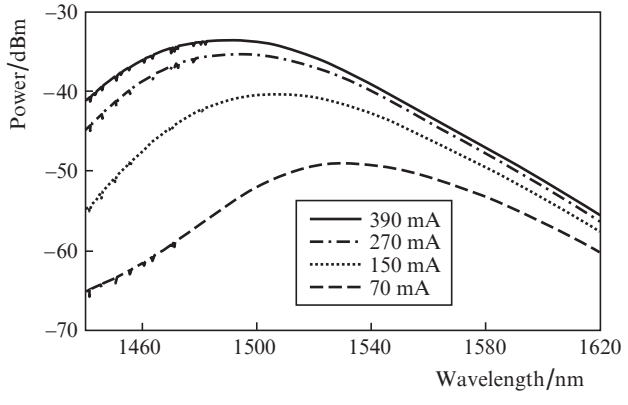

Figure 3. ASE spectra of the ultra-wide band SOA at different injection currents.

small increase in the drive current will result in a large jump in the power of the ASE spectrum generated. However, as the drive current is increased, the resulting increase in the ASE spectra becomes smaller and smaller; this is because of the limited number of carriers that the SOA can sustain at any given time. As such, at the lower drive currents, an increase in the drive current will translate into the significant generation of carriers in the SOA. However, at higher drive currents (approaching the maximum drive current of the SOA) any increase in the drive current generates only few additional carriers. This causes the SOA to operate in a saturated condition and allowing only a slight increase in the power of the ASE spectrum [3]. The second important observation is the shifting of the peak wavelength of the ASE spectra towards the shorter wavelength region as the drive current increases. For instance, at 70 mA, the peak wavelength is approximately 1530 nm, with a higher output power from 1530 nm towards 1620 nm as compared to the power obtained in the shorter wavelength region of 1440 nm to 1530 nm. As the current increases, the peak wavelength shifts towards a shorter wavelength, moving towards 1500 nm and for further increases the wavelength peaks around 1480 nm, with lower output power at the longer wavelengths (from 1520 nm to 1620 nm). This occurs as a result of the distribution of the carrier densities; at lower input powers, the carrier density has a symmetrical spatial distribution, peaking at the centre of the SOA and tailing off towards the input and output facets, thus causing the ASE to peak at the centre region. This is the same characteristic as observed in the case of black body radiation [17].

Figure 4 shows the power of the superluminescent output wavelengths in the S–C–L superluminescent source at different drive currents. The generation of the three, well defined superluminescent wavelengths is achieved when the SOA is operated at a high drive current, for instance at 270 mA, and the VOA is used to adjust the output power of the C- and L-band wavelengths such that the power level is the same as that of the S-band wavelength. Subsequently, the characteristic measurements are done by driving the SOA at low drive currents and increasing the current. It must be noted that the VOA can be fine-tuned to have all three wavelengths with equal power. At the lowest drive current of 70 mA, three superluminescent wavelengths are obtained at 1500, 1540 and 1580 nm, with respective peak powers of –58, –56 and –53 dBm.

As the SOA drive current is increased to 170 mA, the superluminescent wavelength obtained at the S-band (1500 nm) increases only marginally to –42 dBm, whereas the superluminescent wavelengths at the C-band and L-band (1540 and 1580 nm) increase significantly, to –16 and –12 dBm, respectively. A further increase in the SOA drive current to 270 mA brings the three superluminescent wavelengths to –12, –11 and –10 dBm respectively for the wavelengths of 1500, 1540 and 1580 nm. At the highest SOA drive current of 390 mA, there is an increase in the S-band output power, from –12 dBm (270 mA) to –6 dBm, whereas for the case of the C- and L-bands the power remains relatively unchanged. These results are taken without any adjustment to the VOA. The increase in the output power in the shorter wavelength region is due to the ASE spectrum as given in Fig. 3, which has a broad peak towards the shorter wavelength as the drive current increases. The average signal-to-noise ratios (SNRs) of the three generated wavelengths at the lowest drive current of 70 mA is approximately 20 dB, and as the drive current increases to 170, 270 and finally 370 mA, the average SNR also increases to 48, 60 and 62 dB respectively. This correlates with the increase in the superluminescent wavelengths output power at different drive currents. It can also be inferred that the change in the SNR is not linear: It faster at low drive currents, whereas its increase at higher drive currents is only marginal.

Figure 5 shows the measured power as a function of the SOA drive current at different wavelength regions. It can be seen that the C- and L-bands have a lower threshold current of 70 mA, whereas the threshold current for the S-band region is higher at 170 mA.

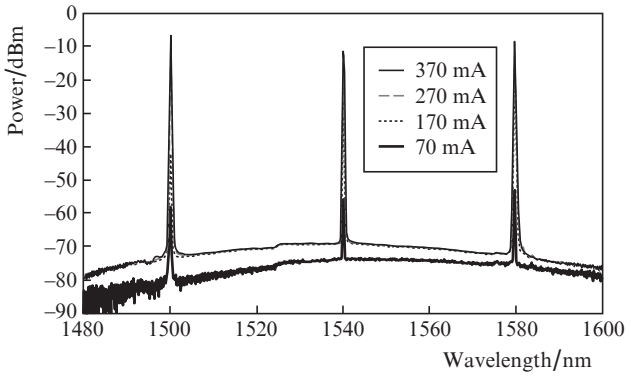

Figure 4. Simultaneous generation of the triple wavelength output at the S-, C- and L-band at different SOA drive currents.

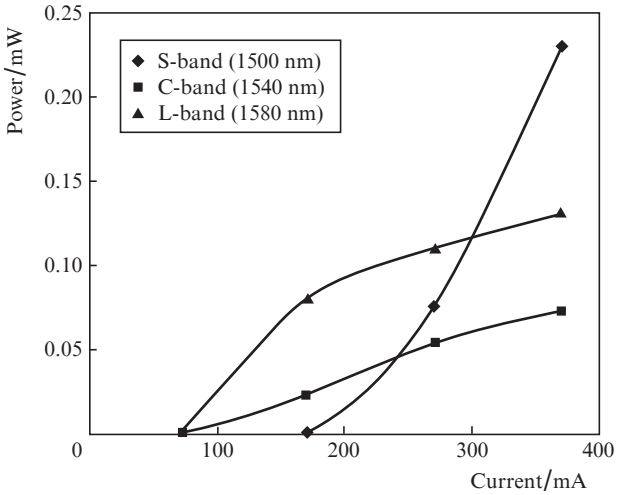

Figure 5. Output power of the SOA as a function of the drive current at different operating wavelengths.

Also, the L-band signal shows a steeper power slope of 8.0×10^{-4} mW mA^{-1} as compared to the plot of the C-band signal, which has a slope of 2.4×10^{-4} mW mA^{-1}. However, at about 170 mA, the slope of the L-band signal plateaus off with a value of about 2.5×10^{-4} mW mA^{-1}. The S-band signal on the other hand has a higher threshold value of 170 mA as compared to the C- and L-band signals, as well as a slope of approximately 7.5×10^{-4} mW mA^{-1} for the region between 170 and 270 mA. However, the slope efficiency of the S-band signal increases significantly to 1.5×10^{-3} mW mA^{-1} after a drive current of 270 mA. At the lower drive currents, the L-band signal initially gives the highest output power, followed by the C-band signal and finally the S-band signal. However, at approxi-

mately 235 mA, the power of the S-band signal increases to equal the power of the C-band signal. At about 280 mA, the S-band signal now becomes as strong as the power of the L-band signal, and at higher drive currents the S-band signal now becomes the dominant signal, with a peak power of almost double the L-band signal and three times larger than that of the C-band signal.

Figure 6 shows the stability of the proposed triple wavelength superluminescent source over a period of 70 minutes, with the spectrum of the lasing wavelengths obtained in 10-minute intervals.

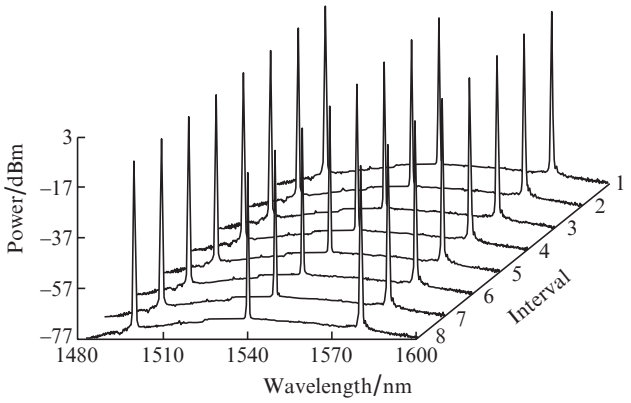

Figure 6. Stability test for the triple wavelength superluminescent source in 10 min time interval. $P_{REF} = -17$ dBm.

It can be seen that the proposed system is highly stable, with minimal fluctuations of less than 3 dB over the test period. As such, the proposed superluminescent source can be used as a viable source for applications such as communications and sensing.

4. Conclusions

A triple-wavelength superluminescent source based on a wide-band SOA and operating in the S-, C- and L-band regions is proposed and demonstrated. The proposed superluminescent source utilises a wide-band SOA with a broad amplification range of 1440 to 1620 nm as the gain medium, and three FBGs at 1500, 1540 and 1580 nm to generate the superluminescent wavelengths. The ASE generated by a ultra-wideband SOA which has a peak power of –49 dBm at 1540 nm at the lowest drive current and a peak power of –33 dBm at 1486 nm at the highest SOA drive current, thereby indicating a wavelength down-shift as the drive current increases. This is attributed to the distribution of the carrier densities in the SOA, akin to black-body radiation. The power of the lasing wavelengths also increases as the drive current is increased, with the wavelengths at 1540 nm and 1580 nm initially increasing faster than the lasing wavelength at 1500 nm. However, at high drive currents, the 1500 nm wavelength is observed to have the highest output power of –6 dBm, while the 1540 and 1580 nm wavelengths have output powers of –11 and –10 dBm respectively, thereby becoming the dominant wavelength. All wavelengths show a good average SNR of more than 60 dB at the highest drive current of 390 mA. The system also shows a high degree of stability, with power fluctuations of less than 3 dB over a time period of 70 minutes. Therefore, the proposed system will have many applications in tasks such as communications and sensing, where a wide-band and stable SOA-based MWSS can be applied.

Acknowledgements. We would like to thank the University of Malaya for providing the funding this project under the UMRG Grants RP019-2012A and RG143-12AET.

References

1. Lee S.L., Jang I.F., Wang C.Y., Pien C.T., Shih T.T. *IEEE J. Sel. Top. Quantum Electron.*, **6**, 197 (2000).
2. Zhang A., Liu H., Demokan M.S., Tam H.Y. *IEEE Photonics Technol. Lett.*, **17**, 2535 (2005).
3. Ahmad H., Thambiratnam K., Sulaiman A.H., Tamchek N., Harun S.W. *Laser Phys. Lett.*, **5**, 726 (2008).
4. Achaerandio E., Jarabo S., Abad S., Amo M.L. *IEEE Photonics Technol. Lett.*, **11**, 1644 (1999).
5. Chaudhari A.L., Shaligram A.D. *Sensors and Actuators A: Phys.*, **100**, 160 (2002).
6. Ye W., Liu W., Chen T., Yang D.Z., Shen Y.H. *Laser Phys.*, **20**, 1636 (2010).
7. Fu J., Chen D., Sun B., Gao S. *Laser Phys.*, **20**, 1907 (2010).
8. Harun S.W., Rahman F.A., Dimyati K., Ahmad H. *Laser Phys. Lett.*, **3**, 495 (2006).
9. Islam M.N., Hwang S., Song K.W., Song K.U., Park S.H., Nilsson J., Cho K. *Electron. Lett.*, **37**, 1539 (2001).
10. Zhou Y.W. *Laser Phys.*, **22**, 753 (2012).
11. Liu X., Zhao W., Liu H., Zou K., Zhang T., Lu K., Sun C., Wang Y., Ouyang X., Chen G., Hou X. *J. Opt. A: Pure Appl. Opt.*, **8**, 601 (2006).
12. Shahabuddin N.S., Harun S.W., Zulkifli M.Z., Thambiratnam K., Ahmad H. *J. Modern Opt.*, **55**, 1345 (2008).
13. Im J.E., Kim B.K., Chung Y. *Laser Phys.*, **21**, 540 (2011).
14. Chen D., Qin S. *Microwave Opt. Technol. Lett.*, **49**, 2339 (2007).
15. Zulkifli M.Z., Jemangin M.H., Harun S.W., Ahmad H. *Laser Phys.*, **21**, 1633 (2011).
16. Ahmad H., Saat N.K., Harun S.W. *Laser Phys. Lett.*, **2**, 369 (2005).
17. Connelly M.J. *IEEE J. Quantum Electron.*, **37**, 439 (2001).